Brønsted Acid-Base Ionic Liquids as Proton Conducting Non-Aqueous Electrolytes

수소이온을 전도하는 무수화
전해질로 브론스테드 산-염기
이온 액체

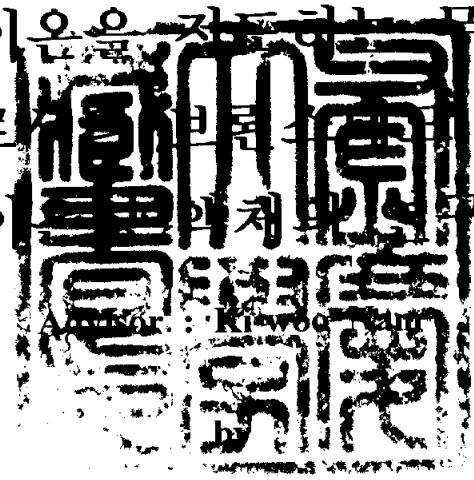

Migyung Yoo

A thesis submitted in partial fulfillment of the requirements
for the degree of
Master of Engineering
in Department of Materials Science and Engineering, Graduate School,
Pukyong National University

February 2004

for the Degree of Master of Engineering

A Dissertation

by

Migyung Yoo

Approved as to style and content by :

Chairman Bong Lee

Member Young-il Kim

Member Ki-woo Nam

December 26 2003

Contents

Brønsted Acid-Base Ionic Liquids as Proton Conducting Non-Aqueous Electrolytes

Migyung Yoo

Department of Materials Science & Engineering
Graduate School of Pukyong National University

Abstract

A super-strong acid, bis(trifluoromethanesulfonyl)amide was combined with 4,4-trimethylene dipyridine(TMDP) and pyridine(PDN) at various molar ratios to prepare a novel series of Brøsted acid-base ionic liquids. The protic neutral salt was electroactive for H_2 oxidation and O_2 reduction at a platinum electrode under non-humidifying condition, which shows the potential of pyridinal systems as new fuel cell electrolytes for elevated temperature operation and foretells the polymeric model of solid-state anhydrous proton conductor.

1. Introduction

1.1 Background of Fuel Cell Study

1.1.1 Basic Principles of Fuel Cells

A fuel cell is another example of a chemical source that may provide electrical energy. It generates an EMF (electro-motive-force) only as long as the oxygen and hydrogen fuel are fed to it.

If a dc voltage is applied to two platinum electrodes immersed in water, the current that flows decomposes the water into its basic parts of hydrogen and oxygen. This is called electrolysis. Hydrogen gas accumulates around the negative cathode and oxygen gas around the positive anode. In chemical terms:

$$2H_2 + \text{electricity} \leftrightarrow 2H_2 + O_2$$

The equation is reversible. This means that the combination of hydrogen and oxygen, in same suitable reaction, should produce water plus electricity. That is,

$$2H_2 + O_2 \leftrightarrow 2H_2O + \text{electrical energy}$$

It can be mentioned more easily with a cell based around an acid electrolyte that is the simplest and still the most common type. At

the anode of an acid electrolyte fuel cell the hydrogen gas ionizes, releasing electrons and creating H^+ ions (or protons),

$$2H_2 \rightarrow 4H^+ + 4e^-$$

At the cathode oxygen reacts with electrons taken from the electrode, and H^+ ions from the electrolyte, to form water.

$$O_2 + 4e^- + 4H^+ \rightarrow 2H_2O$$

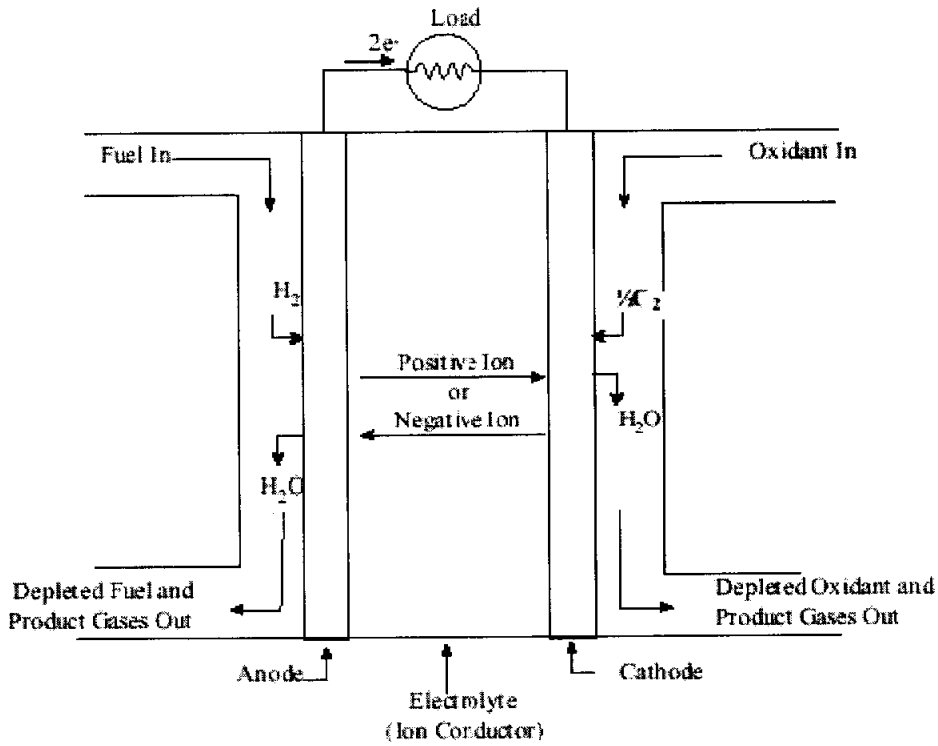

Figure 1.1 Schematic of an Individual Fuel Cell

It should be noted that the electrolyte must only allow H^+ ions to pass through the electrolyte, not round the external circuit, and all would be lost.

It is quite well known that fuel cells are not subject to the Carnot efficiency limit. Because fuel cells convert chemical energy directly to electrical energy, this process does not involve conversion of heat to mechanical energy. Therefore, fuel cell efficiencies can exceed the Carnot limit. A more suitable statement for understanding difference between the theoretical efficiency of fuel cells and heat engines is that if a fuel cell is compared to an equivalent efficiency heat engine, the fuel cell is not limited by temperature as is the heat engine. The freedom from temperature limits of the fuel cell provides a great benefit because it relaxes material temperature problems when trying to achieve high efficiency.

In the ideal case of an electrochemical converter, such as a fuel cell, the change in Gibbs free energy, ΔG of the reaction is available as useful electric energy at the temperature of the conversion. The ideal efficiency of a fuel cell, operating irreversibly, is then

$$\eta = \frac{\Delta G}{\Delta H}$$

The most widely used efficiency of a fuel cell is based on the change in the standard free energy the cell reaction,

$$H_2 + 1/2\ O_2 \rightarrow H_2O(1)$$

given by

$$\Delta G^0_r = G^0_{H_2O(l)} - G^0_{H_2} - \frac{1}{2} G^0_{O_2}$$

where the product water is in liquid form. At standard conditions of 25℃(298**K**) and 1 atmosphere, the chemical energy ($\Delta H = \Delta H_o$) in the hydrogen/oxygen reaction is 285.8 kJ/mole, and the free energy available for useful work is 237.1 kJ/mole. Thus, the thermal efficiency of an ideal fuel cell operating reversibly on pure hydrogen and oxygen at standard conditions would be:

$$\eta_{ideal} = \frac{237.1}{285.8} = 0.83$$

The efficiency of an actual fuel cell can be expressed in terms of the operating cell voltage to the ideal cell voltage. The actual cell voltage is less than the ideal cell voltage because of the losses associated with cell polarization and iR loss. The thermal efficiency of the fuel cell can then be written in terms of the actual cell voltage,

$$\eta = \frac{Useful\ Energy}{\Delta} = \frac{Useful\ Power}{(\Delta G/0.83)}$$

$$= \frac{Volts_{actual} \times Current}{Volts_{ideal} \times Current/0.83}$$

$$= \frac{(0.83)(V_{actual})}{V_{actual}}$$

As mentioned, the ideal voltage of a cell operating reversibly on hydrogen and oxygen at 1 atm pressure and 25℃ is 1.229V. Thus, the thermal efficiency of an actual fuel cell operating at a voltage of V_{cell}, base on the higher heating value of hydrogen, is given by

$$\eta_{ideal} = 0.83 \times V_{cell} / V_{ideal} = 0.83 \times V_{cell} / 1.229 = 0.675 \times V_{cell}$$

A fuel cell can be operated at different current densities, expressed as mA/cm^2 or A/ft^2 . The corresponding cell voltage then determines the fuel cell efficiency. Decreasing the current density increases cell voltage, thereby increasing the fuel cell efficiency.

1.1.2 Fuel Cell Types and Main Advantages

Table 1.1 Data for different types of fuel cell

Fuel Cell type	Mobile Ion	Operating Temp.	Application and Notes
① Alkaline- AFC	OH^-	50 ~ 200℃	Used in space vehicles, e.g. Apollo, shuttle.
② Proton Exchange membrane (PEM)	H^+	50 ~ 100℃	Suitable for vehicles and mobile applications. but also for lower CHP systems.
③ phosphoric acid (PAFC)	H^+	~ 220℃	Large numbers of 200kW CHP system in use.
④ Molten carbonate (MCFC)	CO_3^{2-}	~ 650℃	Suitable for medium to large scale CHP systems, up to MW capacity
⑤ Solid oxide (SOFC)	O^{2-}	500 ~ 1000℃	Suitable for all sizes of CHP systems 2kW to multi MW.

cf. CHP(combined heat and power): feature enables the system to capture the heat generated during the production of electricity and utilize it for facility heat or hot water.

Most of the notable achievements of AFCs have been using pure hydrogen and oxygen supplies for air as independent power sources. However, the scope for these is limited.

The main problem with AFCs for terrestrial applications is the problem of carbon dioxide reactions with the alkaline electrolyte. This occurs with carbon dioxide in the air. So the OH^- concentration is reduced, thus reducing the ratio of reaction at the anode. And the viscosity is increased, reducing the diffusion rates, thus lowering the limiting currents and increasing the mass transport losses.

The PAFC was the first to be produced in commercial quantity and enjoy widespread terrestrial use. Many 200kw systems, manufactured by International Fuel Cells Corporation, are installed in the USA and Europe, as well as systems produced by Japanese companies.

Porous electrode, platinum catalysts and a fairly high temperature (< 220℃) are used to boost the reaction rate to a reasonable level.

The hydrogen fuel is solved by 'reforming' natural gas (CH_4, mathane) to hydrogen and carbon dioxide, but the equipment needed to do this adds considerably to the cost, complexity and size of the fuel cell.

The MCFC has the interesting feature that it needs the carbon dioxide in the air to work. Even though the operating temperature in the MCFC is high (< 650℃), its good reaction rate is achieved using a comparatively inexpensive catalyst-nickel. The nickel also forms the electrical basis of the electrode. Like the SOFC it can use gases such as methane and coal gas (H_2 and CO) directly without an external reformer. However, this simplicity is somewhat offset by the nature of the electrolyte, a hot and corrosive mixture of lithium, potassium and sodium carbonates.

The SOFC operates in the region of 600 to 1000℃. This means that high reaction rates can be achieved without expensive catalysts and that gases such as natural gas can be used directly, or 'internally reformed' within the fuel cell without the need for a

separate unit. This fuel cell type thus addresses all the problems and takes full advantage of inherent simplicity of the fuel cell concept. Nevertheless, the ceramic materials that these cells are made from are difficult to handle, so they are expensive to manufacture and there is still a large amount equipment needed to make a full fuel cell system. This extra plant includes air and fuel pre-heaters, also the cooling system is more complex and they are not easy to start up. Despite operating at temperatures up to 1000℃, the SOFC always stays in the solid state.

The PEM fuel cell capitalizes on the essential simplicity of the fuel cell. The electrolyte is a solid polymer, in which protons are mobile with a solid and immobile electrolyte. This type of cell is inherently very simple.

This cell runs at quite low temperature so the problem of slow reaction rates is addressed by using sophisticated catalysts and electrodes. The problem of hydrogen supply is not really addressed- quite pure hydrogen must be used, though various ways of supplying this possible.

1.1.3 Feature of PEMFC(PEFC)

The basic cell in the PEFCs system consists of a proton conducting membrane, such as a perfluorinated sulfonic acid polymer, sandwiched two platinum impregnated porous electrodes. The back of the electrodes is made hydrophobic by coating with an appropriate compound, such as Teflon. This wet proof coating provides a path for gas diffusion to the catalyst layer. Because of the intrinsic nature of materials used, low temperature operation of approximately 80℃ is possible. The cell is also able to sustain operation at very high current densities. For comparing fuel cell electrodes and electrolytes the main figure is current per unit area, such as the current density. This is usually given in $mA \cdot cm^{-2}$. This figure should be given at a specific operating voltage, typically about 0.6 or 0.7 volt. These attributes lead to a fast start capability and ability to make a compact and lightweight cell. As a result the PEFC is particularly suited for vehicular power application.

Transportation applications mean that the fuel of choice will probably be methanol although hydrogen storage on-board in the form of pressurized gas and the partial oxidation of gasoline is being considered. The cell is also considered for smaller scale stationary power application, which will use natural gas or other hydrogen-rich gases. The lower operating temperature of a PEFC results in both advantages and disadvantages. Low temperature operation is

advantageous because the cell start from ambient conditions quickly, especially when pure hydrogen fuel is available.

It is a disadvantage in that platinum catalysts are required to promote the electrochemical reaction. Carbon monoxide (CO) binds strongly to platinum sites at temperatures below 150℃, which reduces the sites available for hydrogen chemisorption and electro-oxidation. The most important disadvantage of fuel cell at the present time is high cost. However, there are many advantages, especially following the wold wide currency.

As a summary of it including other type fuel cells, first is the efficiency. Fuel cells are generally more efficient than combustion engines. For instance, the value of the efficiency limit relative to the higher heating value, for a hydrogen fuel cell reaches at 83%. The efficiency equation was already elucidated.

A further feature of this is that small systems can be just as efficient as large ones. This is very important in the case of the small local power generating systems needed for combined heat and power systems.

Secondly is simplicity. The essentials of a fuel cell are very simple without moving parts in the energy converter. This can lead to highly reliable and long systems.

Thirdly is low emissions. The by-product of the main fuel cell reaction, when hydrogen is the fuel, is pure water, which means a fuel cell can be essentially "zero emission". This is main advantage

when used in vehicles, however, it should be noted that, at present, emission of CO_2 is nearly always involved in the production of the hydrogen needed as the fuel.

Lastly is silence. Fuel cells are very quiet even those with extensive extra fuel processing equipment. This is very important in both portable power applications and for local power generation in CHP schemes.

1.2. The Concept and the Aim in this Study

The need for an efficient, non-polluting power source for vehicles in urban environments has resulted in increased attention to the option of the fuel cell powered vehicles. The polymer electrolyte fuel cell(PEFC) technology seems to be fittest for terrestrial transportation applications. A significant number of PEFCs employ perfluoro sulfonate ionomer typically Nafion® as their electrolyte.

As mentioned above, the greatest barrier commercialization on a large scale is the high cost of the cell components, including the membrane and platinum. And PEFCs are especially vulnerable to "flooding": the membrane becomes over-wet due to production of water at the cathode and diffusion of reaction is blocked. The catalytic activity of Pt electrode decreases for the poisoning by CO, necessitating the elevated temperature operation. But the high temperature operation is restricted for the evaporation of water, which results in significant decrease in ionic conductivity.

We have therefore focused our attention to replace the proton carrier, H_2O with organic amines, which can be operated at high temperature under anhydrous condition.[1]

In this study, it will be shown that pyridine and dipyridinal conjugate, 4,4-trimethylene dipyridine(TMDP) as Brøsted bases were used for obtaining ionic liquids under non-humidifying condition by simple combination with a super strong acid bis(trifluoromethanesul-

fonyl)amide(HTFSI) and electrochemically provide insight into the proton conduction.

2. Experimental

2.1 Materials

Bis(trifluoromethanesulfonyl)amide(HTFSI) (Morita Chemical Industries 99.8%) was used as a super strong acid. 4,4-trimethylene dipyridine(TMDP) and pyridine(PDN) as bases were used to mix with HTFSI in the various ratios. Chemical structures of HTFSI as a acid, TMDP and PDN as bases are shown in Figure 2.1

Appropriate amounts of HTFSI and TMDP maintaining defined molar ratios were mixed and heated above the respective melting points. As PDN is exposed in the air, it is immediately volatile. So the mixture of HTFSI and PDN was just stirred on a stirring plate. All the samples were handled and stored in argon atmosphere glove box (VAC, $[O_2] < 1ppm$, $[H_2O] < 1ppm$)

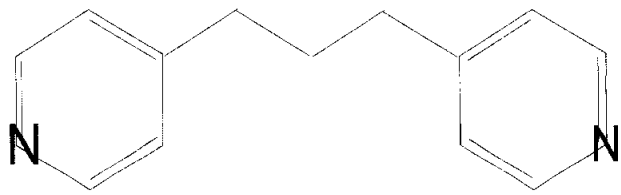

TMDP(base)

m.p. 57℃

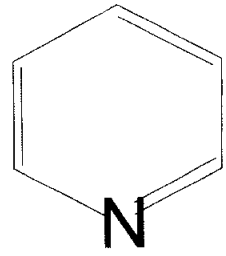

PDN(base)

m.p. -42℃

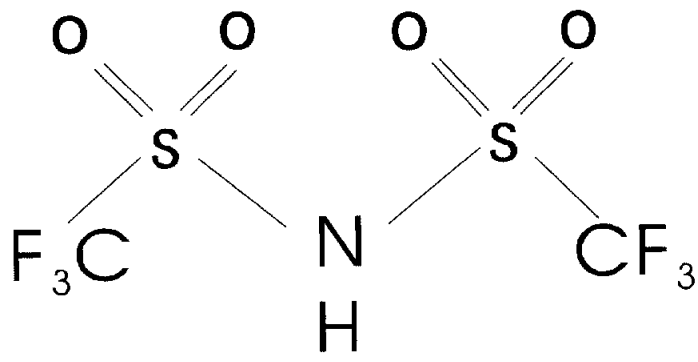

HTFSI(acid)

m.p. 52℃

Figure 2.1 Molecular Structure

2.2 Measurement

2.2.1 Thermal Property

High-temperature stabilities for the samples were measured on a thermo-gravimetry/differential thermal analyzer (TG/DTA6200. Seiko Instruments) from 35 to 550℃ at a heating rate of 10℃min^{-1} under air atmosphere with open Al pans. The sample weight being put on open Al pans was between 10mg and 20mg. Calcium oxalate monohydrate, $CaC_2O_4.H_2O$ was used as a standard for the calibration of the thermo-gravimetric changes.

Differential scanning calorimetry (DSC) was carried out with DSC220C (Seiko Instruments) under N_2 atmosphere. The calibration of temperature and heat capacity was made by using cyclohexane, indium and tin as standards. The samples for DSC measurements were tightly sealed by using a device for sealing Al pans in a glove box. Thermograms were recorded during cooling (25 to -150℃) scans, followed by heating (-150 to a temperature close to the deco-mposition temperature at around 200℃) scans in [TMDP]/[HTFSI] system. In [PDN]/[HTFSI] system, it was also carried out in same way but setting points were different. Because [PDN]/[HTFSI] system has only one melting point above 0℃ (57.3℃), which exists in 5:5 composite. So, in [PDN]/[HTFSI] system, thermogrms were recorded during heating (-150 to 90℃) scans. The glass transition temperature (T_g: onset of the heat capacity change), crystallization

temperature (T_c: onset of the exotherm peak), melting temperature (T_m: onset of the endotherm peak), and melting temperature of the eutectic mixture (T_e: onset of the endotherm peak) were determined from DSC thermograms during the heating scans.

2.2.2 Ionic Conductivity

The ionic conductivity was determined using the complex impedance method in the temperature range of 60 to 130℃ (ESPES temperature chamber SU-220). The samples were thermally equilibrated at each temperature for at least 1h prior to the measurements. When samples especially solid types are put into the cell for measuring, thanks to the transparent cell, it is useful for observing samples' transition such as a change of colors, melting degree, etc. ESPES temperature chamber SU-220 (limit temperature 150℃) is a tightly-shut type, invisible inside for measuring. One temperature set after another temperature step, just for a second, with opening the chamber, samples condition could be checked. As this reason, another type chamber (Yashima, BX-10, limit temperature 300℃) with a clear square window on the door was used, of course it is convenient for many things especially increasing temperature, but the reliance of the measurement was somewhat low and its result was scrapped except for the melting condition of samples and changing colors following each temperature. A set of the cell consists of one glass tube (diameter 7mm, copper electrodes), a Teflon washer of handiwork and a glass cover. The samples (electrolytes) were filled up glass cells with the cover fitted and were sealed up between the cover and the washer with a Teflon® tape in the glove box. The cell constant determined by 0.1

M KCl standard solution (Kanto Kagaku) was 0.52cm^{-1} at 25℃. The experiments were carried out with a computer-interfaced Hewlett-Packard 4192A LF impedance analyzer over the frequency from range 5Hz to 13 MHz.

2.2.3 Electrochemical Polarization (Fuel Cell Test)

The measurements were performed with using a two-compartment glass cell (Fig. 2.2) in a Solartron electrochemical interface at 130℃ for [TMDP]/[HTFSI]=1/2 salt. The working electrode (W.E.) and reference electrode(R.E.) in this experiment were coil-shaped Pt-wire(0.5 diameter, 4.5cm length) and the counter electrode was a coil-shaped Pt-black wire. The W.E. was set under a O_2 gas bubbling atmosphere, while the C.E. was under a H_2 gas bubbling atmosphere. The Pt-wire in a H_2 atmosphere worked as a reversible hydrogen electrode (RHE^2). The electrodes were treated by repetitious cathodic and anodic polarization in 2M H_2SO_4 solution before every experiment. Surface area of the working electrode was estimated from H_2 adsorption-desorption value of 1M H_2SO_4 solution at 30℃ in Ar atmosphere. In all of the experiments, the electrode and gas tubes were mounted into the glass cells with a Swagelok® tube connector. The electrochemical control was accomplished using a Solarton electrochemical interface (model 1287). All data were collected and analyzed on a PC with commercial CorrWare 2 and CorrView software (Scribner Associates Inc.) respectively. The temperature was regulated by using a constant temperature chamber (Yashima, BX-10).

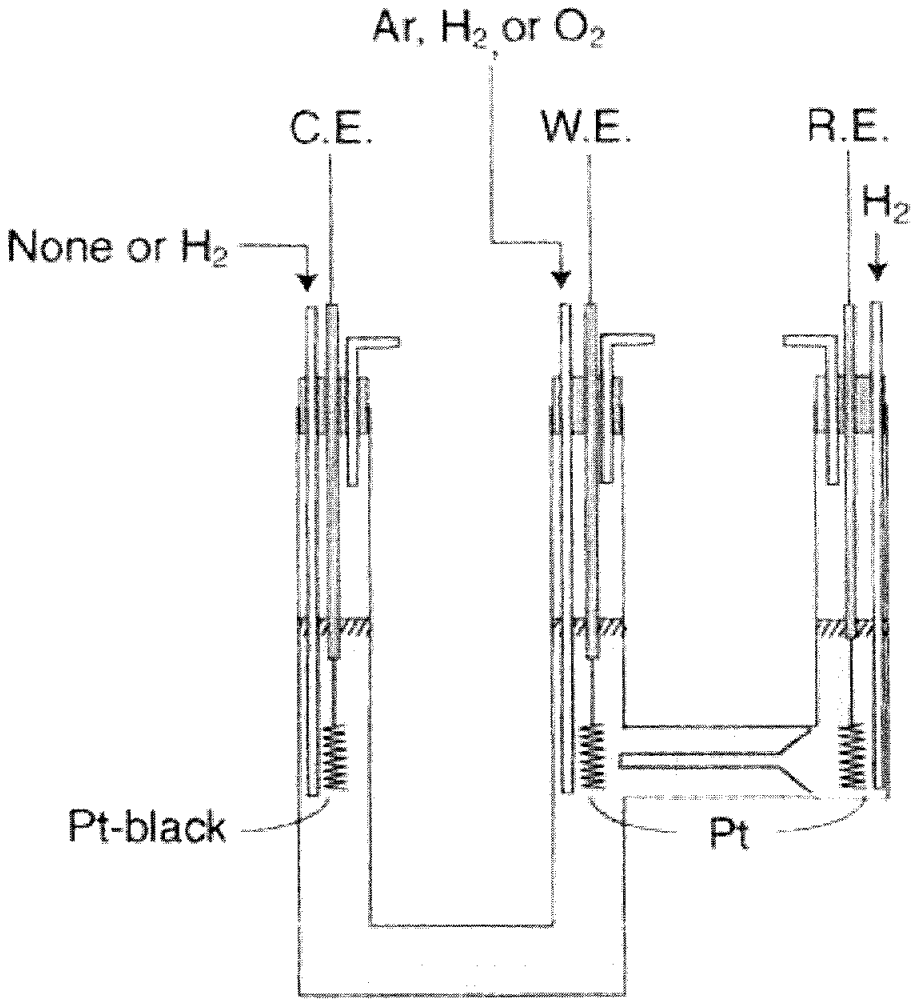

Figure. 2.2 Scheme Of Proton Pump Cell

3. Results and Discussion

The thermal properties of various compositions for [TMDP]/[HTFSI] system and [PDN]/[HTFSI] system have been summarized in Table 3.1, 3.2. The melting temperature, T_m of the [TMDP]/[HTFSI] = 1/2 composition is 62.0℃, while that of the [TMDP]/[HTFSI] = 1/1 composition is 160.0℃. The T_m in the [TMDP]/[HTFSI] system varied with the composition change.

In Table 3.1 the eutectic point exists at 57.1℃ for the compositions between a salt with the composition of [TMDP]/[HTFSI] = 1/1 and neat TMDP, showing the typical behavior of a binary mixture. The fact that T_m of the compositions increases from the corresponding value of the [TMDP]/[HTFSI] = 1/2 until the composition reaches [TMDP]/[HTFSI] = 1/1, may be ascribed to the strong interaction from intermolecular H-bond between the pyridine moiety in TMDP and the protonated counterparts. Some of compositions, [TMDP]/[HTFSI] = 8.5/1.5, 9/1, 9.5/0.5, become supercooled easily at ambient temperature.

The thermogravimetric (TG) curve of the [TMDP]/[HTFSI] = 1/2 composition shows a single-step weight loss process like that of neat TMDP (Figure 3.1) This indicates that the formed salt has very high thermal stability up to 392.0℃. On the contrary, the TMDP-rich compositions show two-step weight loss processes.

In discussion of the [PDN]/[HTFSI] (Figure 3.2, Table 3.2),

especially in its thermal property, the eutectic point can be regarded at around -57.8℃ between the 9/1 composition and the 9.7/0.3 composition

In Figure 3.3 TG curve of the [PDN]/[HTFSI] system nearly shows two-step. According to decomposition temperature of 1/1 composition, 329.5℃, this neutral salt also has very high thermal stability. But as it goes on rich base composition, it tends toward sharp gradient. It can be mentioned this comes from pyridine and for the most part this system is unstable at ambient temperature. All of the compositions are liquids except for 1/1 composition after mixture.

Figure 3.4 shows the Arrhenius plots of which ionic conductivities for neutral salt of PDN and TMDP with HTFSI along with some base rich [TMDP]/[HTFSI] compositions. As it can be seen in Figure 3.4 the neutral salt of [PDN]/[HTFSI] = 1/1 has much higher ionic conductivity compared to that of TMDP. This is due to the higher ionic mobility of small pyridinium cation [PDN^+] compared to the large trimethylene dipyridinium cation [$TMDP^+$].

In regard to [TMDP]/[HTFSI], for the base-rich composition of [TMDP]/[HTFSI] = 7.5/2.5, the ionic conductivity is higher than the value of [TMDP]/[HTFSI] = 1/2 composition (Figure 3.4) Since the number of ion carriers, H_2TMDP^{2+} and $TFSI^-$ are maximum at [TMDP]/[HTFSI] = 1/2 composition, the increase in ionic conductivity with increase in mole fraction of TMDP indicates enhanced ionic mobility, which is also confirmed by the lower Ea

values (Figure 3.5). The conductivity therefore may be due to not only to ionic species like H_2TMDP^{2+}, $HTMDP^{2+}$ and $TFSI^-$, but also to intermolecular proton transfer. The conductivity measurements for other compositions with 7/3≥ [TMDP]/[HTFSI] ≥ 3.6 could not be conducted due to their high melting points with our present available. The ionic conductivity of neat TMDP is significantly low in the temperature range studied.

The activation energies, *E*a of different compositions were calculated from temperature dependance of ionic conductivity from 60 ℃ to 130℃ in the liquid state of the system using Arrhenius equation (Figure 3.6). For the compositions studied, *E*a decreases with increasing mole fraction of TMDP for TMDP rich compositions from the corresponding value for [TMDP]/ [HTFSI] = 1/2 composition, with maximum value for neat TMDP. Since there is no another composition for comparison in [PDN]/[HTFSI] system, only *E*a of a neutral salt was calculated.

To substantiate the protonic conduction, we conducted a simple direct current polarization experiment at 130℃ using a U-shaped glass tube with two pt-wire electrodes (proton pump cell). The anode was under an H_2 or Ar bubbling atmosphere. The current detected under an Ar atmosphere for [TMDP]/[HTFSI] = 1/2 composition was quite low, whereas a noticeable change could be distinguished upon charge to a H_2 gas atmosphere resulting in observation of higher current. This is indicative of following

phenomenon, occurring at the anode, electrolyte, and cathode:

Anode: H_2 + TMDP → H_2TMDP^{2+} + $2e^-$

Electrolyte: proton conduction

Cathode: H_2TMDP^{2+} + $2e^-$ → TMDP + H_2

In fact, evolution of H_2 gas could be observed as bubbles at the cathode for prolonged polarization experiment. It should be noted that the neutral salt without stoichiometric excess of free TMDP exhibited proton conductivity. The elucidation of the proton conduction mechanism in neutral ionic liquid system is now underway. The probable mechanisms include functioning of the imide ion ($TFSI^-$) as a proton acceptor site, translational dynamics of the protonated amines[2] (vehicle mechanism), and hopping through free amines by Grotthuss mechanism[3,4] probably persisting in the system from th e equilibrium between neutral salt and the starting amine and HTFSI (Figure 3.7).

The current vs potential (vs RHE) characteristics of an H_2/O_2 fuel cell under non-humidifying condition has been depicted in Figure 3.8. Although a potential drop with increasing current density is apparent possibly due to the electrode polarization and to some extent to LR drop, this is a clear evidence of electric power generation by an H_2/O_2 fuel cell.

There was reported sharply contrasts to the negative result from

a related material[6]

Despite the fact that TMDP-rich compositions are promising as proton conducting non-aqueous electrolytes for probable proton conduction by fast proton exchange between protonated and free TMDP by structure diffusion[7] (Grotthuss mechanism), as anticipated from the conductivity result, the electrochemical polarization results showed remarkable electrochemical instability at Pt electrodes with increasing free TMDP content in the system.

4. Summary

The TMDP molecule, with two-pyridine groups linked with trimethylene chain in the structure, prognosticates a polymeric model for proton conductor. It is likely that pyridine molecule will retain reasonably high ionic conductivity and ability to conduct proton even in the polymeric state.

This finding is therefore, a herald of a new field of fuel cell under non-humidifying conditions, which may be operated at temperatures above 100℃ and provide a firm underpinning for the development of solid-state anhydrous proton conductors using the concept of ionic liquid.[9]

Table 3.1 Thermal Properties for TMDP/HTFSI composites.

[TMDP]/ [HTFSI]	T_g/℃	T_c/℃	T_e/℃	T_m/℃	T_{d1}/℃	T_{d2}/℃
10/0	-	-	-	63.0	227.2	-
9.5/0.5	-	-	-	59.0	240.0	348.0
9/1	-65.1	-35.5	5.8	57.0	242.0	358.0
8.5/1.5	-	-38.5	-	57.1	245.0	362.0
8/2	-63.8	-36.9	56.9	112.5	225.6	379.5
7.5/2.5	-64.2	-35.4	56.9	125.1	229.0	381.0
7/3	-64.3	-34.9	-	137.0	231.0	385.3
6/4	-65.7	-23	45.5	131.4	244.0	391.0
5.5/4.5	-62.3	-	-	152.2	238.0	389.0
5/5	-	-	-	160.0	291.6	392.0
4.5/5.5	-	-	-	157.0	288.4	391.0
4.2/5.8	-	-	-	-	303.0	398.0
4/6	-	-9.1	58.0	154.0	305.0	396.0
3.6/6.4	-35.4	-10.1	54.0	142.0	-	392.5
1/2	-35.2	9.4	62.0	-	-	392.0

T_g: onset temperature of a heat capacity change (glass transition temperare)

T_c: onset temperature of an exotherm peak (crystallization temperature)

T_e, T_m: onset temperature of an endotherm peak (eutectic temperature, melting temperature). Temperatures above during cooling and heating scans from -150 to 200℃ by using differential scanning calorimetry.

T_d: onset temperature of 10% weight loss during heating scans from room temperature by using thermo-gravimetry.

Table 3.2 Thermal Properties for Pyridine/HTFSI composites.

[Pyridine] / [HTFSI]	T_{g1}/℃	T_{g2}/℃	T_c/℃	T_e/℃	T_m/℃	T_{d1}/℃	T_{d2}/℃	T_x/℃
5 / 5	-70.2	-57.6	-	-	57.3	-	329.5	-
6 / 4	-81.7	-	-49.6	-	-3.6	84.3	335.2	48.6
6.5 / 3.5	-	-76.0	-29.1	-	-3.4	80.5	334.3	44.2
7 / 3	-88.9	-65.4	-51.8	-	-21.1	75.5	344.8	45.6
8 / 2	-108.4	-	-47.6	-	-	61.6	321.4	43.7
8.5 / 1.5	-115	-	-	-	-	93.7	323.3	42.8
9 / 1	-128.8	-	-89.8	-57.8	-	52.6	319.4	43.3
9.3 / 0.7	-	-	-	-54.9	-	56.7	323.5	-
9.7 / 0.3	-	-	-	-46.3	-	-	308.7	44.5
10 / 0	-	-	-	-	-40.9	-	-29.2	46.8

T_g: onset temperature of a heat capacity change (glass transition temperature)
T_c: onset temperature of an exotherm peak (crystallization temperature)
T_e, T_m: onset temperature of an endotherm peak (eutectic temperature melting temperature). Temperatures above during cooling and heating scans from -150 to 200℃ by using differential scanning calorimetry.
T_d: onset temperature of 10% weight loss during heating scans from room temperature by using thermo-gravimetry.

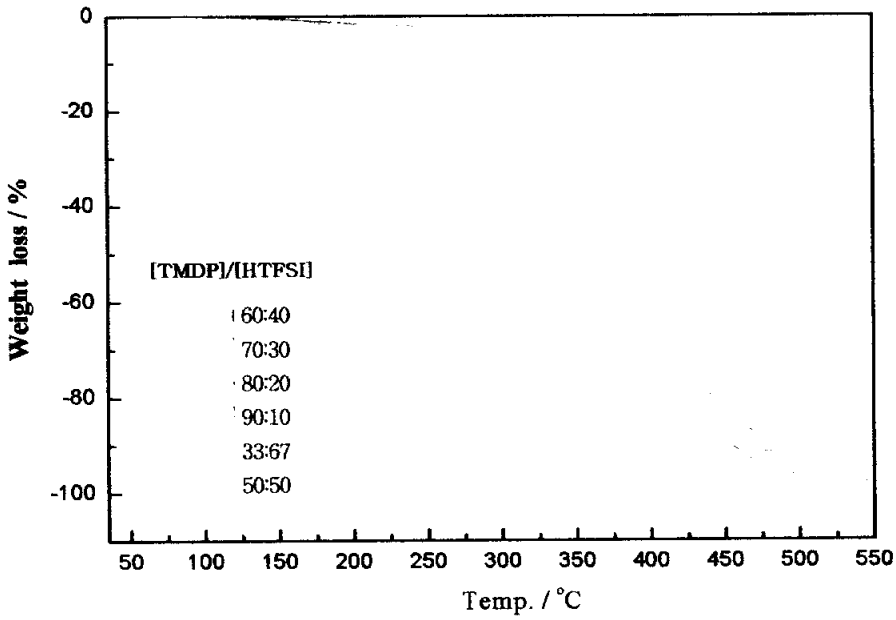

Figure 3.1 TG curves of [TMDP]/[HTFSI] system

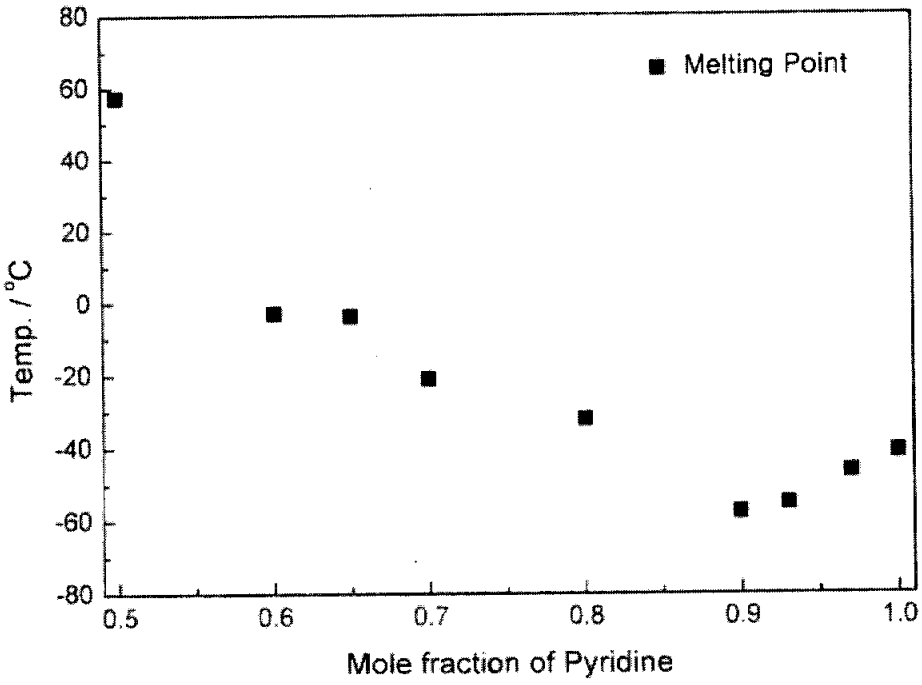

Figure 3.2 Phase diagrams of [PDN]/[HTFSI] system

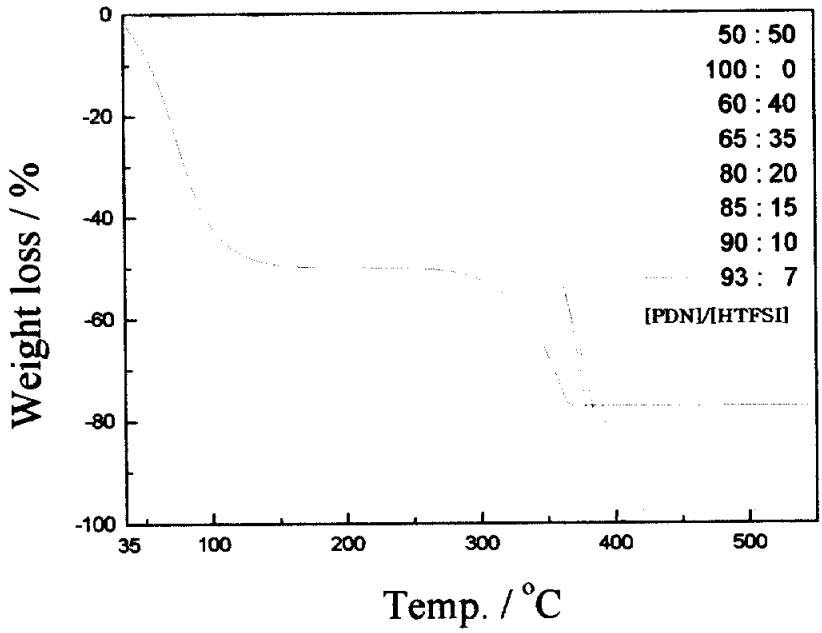

Figure 3.3 TG curves of[PDN]/[HTFSI] system

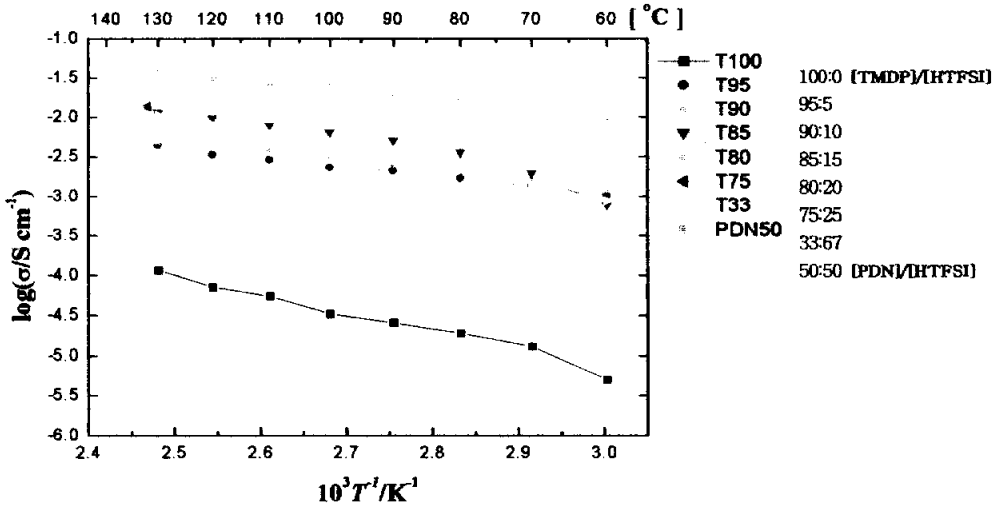

Figure 3.4 Arrhenius Plots of Ionic Conductivity for [TMDP]/[HTFSI] and [PDN]/[HTFSI]

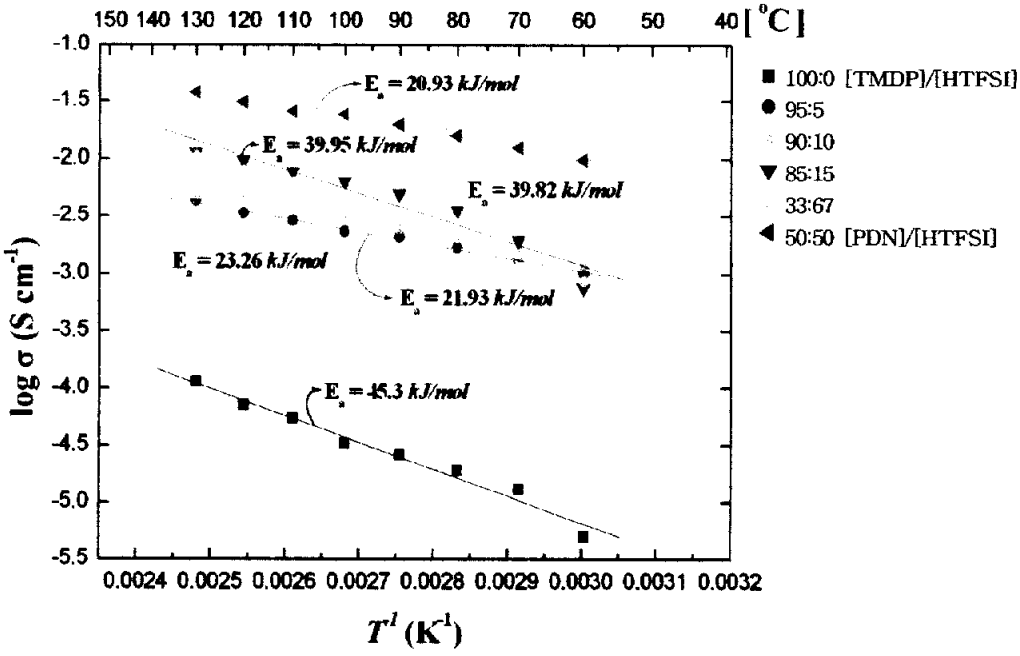

Figure 3.5 Activation Energy Plot of [TMDP]/[HTFSI] and [PDN]/[HTFSI] along with Arrhenius Equation

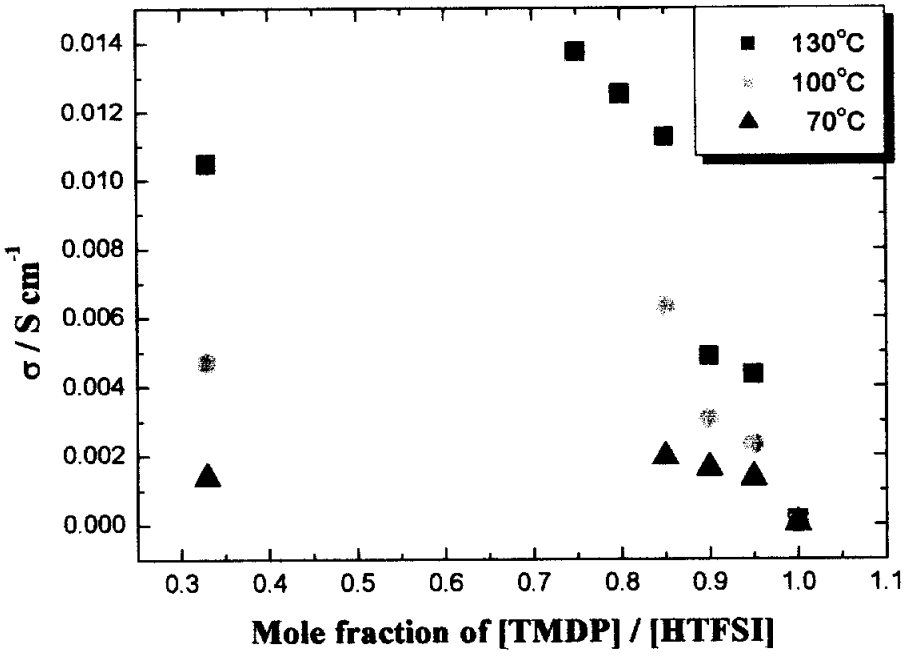

Figure 3.6 Ionic Conductivity as a Function of Mole Fraction of TMDP

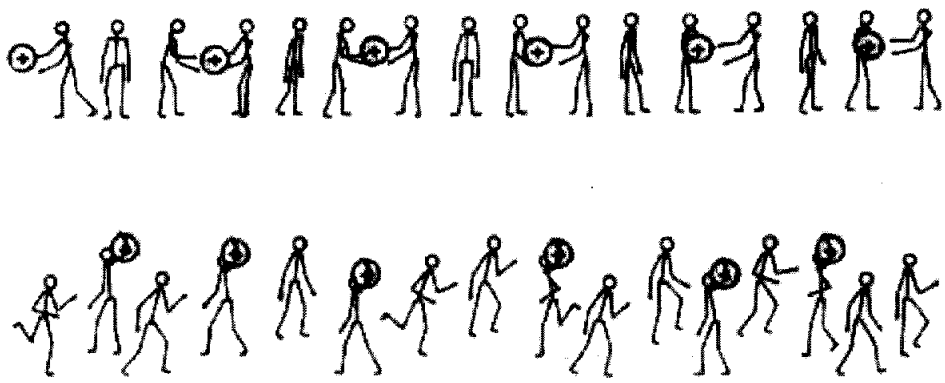

Figure 3.7 Model of Proton Conduction

Top: Grotthuss Mechanism :

The Protons are Passed along the hydrogen bonds.

Bottom : Vehicle Mechanism :

The movement takes place with the aid of a moving "vehicle", e.g. H_2TMDP^{2+} ([TMDP]/[HTFSI] system)

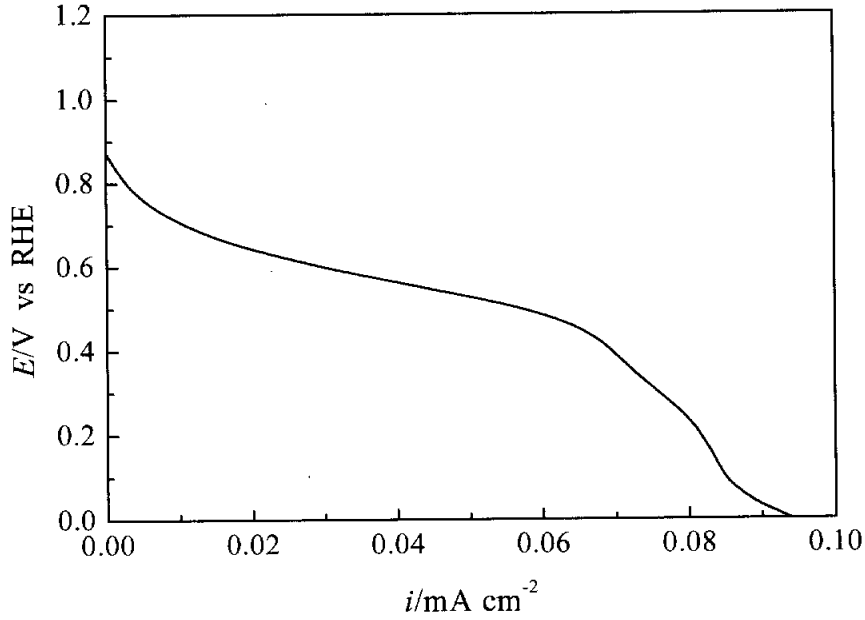

Figure 3.8 Fuel cell characteristics for TMDP/HTFSI = 1/2 composition at 130℃. Scan rate is $10mVs^{-1}$

References

1. a) M. Doyle, S. K. Choi, and G. *Proulx, J. Electrochem. Soc.*, **147**, 34 (2000). b) J. Fuller and R. T. Carlin, *Electrochem. Soc. Proc.*, **41**, 27(1999).

2. A. Noda, M. A. B. H. Susan, K. Kudo, S. Mitsushima, and M. Watanabe, J. Phys. Chem. B, **107**, 4024 (2003).

3. K. D. Kreuer, A. Rabenau, and Wepner, *Angew. Chem., Int. Ed. Engl.*, **21**, 208 (1992)

4. a) K. D. Kreuer, A. Fuchs, M. Ise, Spaeth, and J. Maier, *Electrochem. Acta,* **43**, 1281 (1998). b) M. Schuster, W. H. Meyer, G. Wegner, H. G. Herz, M. Ise, M. Schuster, K. D. Kreuer, and J. Maier, *Solid State Ionics,* **145**, 85 (2001). c) R. Bouchet and E. Siebet, *Solid State Ionics,* **118**, 287 (1999).

5. C. J. D. van Grotthuss, *Ann. Chem.*, **58**, 54 (1806).

6. C. Yang, P. Costamagna, S. Srinivason, J. Benziger, and A. B. Bocarsly, *J. Power Sorces*, **103**, 1 (2001)

7. K. D. Kreuer, *Solid State Ionics,* **136-137,** 149 (2000)

8. A. Noda, M. Watanabe, *Electrochem. Acta,* **45**, 1265 (2000).